PHYSICAL REVIEW B
CONDENSED MATTER

THIRD SERIES, VOLUME 31, NUMBER 12 15 JUNE 1985

Calculated inverse photoemission cross sections from adsorbed molecules

P. D. Johnson and J. W. Davenport
Department of Physics, Brookhaven National Laboratory, Upton, New York 11973
(Received 11 February 1985)

A quantum-theoretical treatment is applied to calculate the cross section for emission of photons produced in inverse photoemission from an adsorbed molecule. Careful consideration of the type of potential that may be used in such calculations shows that photoemission and inverse photoemission from localized levels may be treated as time-reversed processes only above some minimum energy, approximately four times the threshold energy. In situations where time reversal may be used, a simple formula is derived relating the cross sections for photoemission and inverse photoemission. Examination of cross sections shows that the shape resonance frequently observed in photoemission as a final-state effect may manifest itself in inverse photoemission as an initial-state effect.

I. INTRODUCTION

In the last few years inverse photoemission has emerged as a versatile tool for the study of the unoccupied energy levels of both clean and adsorbate-covered surfaces.[1] As the name suggests, inverse photoemission is generally considered as the time reversal of the photoemission process. Thus, an electron incident on the system under investigation may couple into an unoccupied level and then make a transition to a more tightly bound unoccupied level with the emission of a photon. This photon will have an energy given by the energy difference between these initial and final states. Applied to the situation of an atom or molecule we may consider the electron as making a radiative transition between different eigenstates of the negative ion.

Inverse photoemission therefore has much in common with spontaneous emission or the deexcitation of an excited atom or molecule. From the advent of quantum theory it was recognized that while a semiclassical treatment gave a reasonable description of the photoemission process it could not adequately explain the emission of a photon resulting from the deexcitation of an excited atom. If the electromagnetic field is described by a classical vector potential $\mathbf{A}$, the transition matrix element for radiative transitions between two states (mediated by the operator $\mathbf{A}\cdot\mathbf{p}$) should be zero when there is no electromagnetic wave incident on the atom.

This dilemma was removed in 1927 with Dirac's quantization of the electromagnetic field.[2] Dirac was able to give a single theoretical treatment describing both the absorption and emission of photons by an atomic system.

In Sec. II of this paper we review the quantized-field treatment and examine its application to the inverse photoemission process and in Sec. III we show how this method may be applied to give a description of the inverse photoemission observations from molecules oriented on surfaces. In particular we apply the technique to analyze the angle-resolved observations of the unoccupied 2π level of adsorbed carbon monoxide. Our theory is essentially equivalent to that of Pendry, who has previously considered the emission of photons resulting from inverse photoemission processes in the solid-state environment.[3]

II. THEORY

Photoemission and inverse photoemission both involve the interaction between photons and electrons. As usual, the interaction Hamiltonian (neglecting spin) is given by

$$H'=\frac{e}{2mc}(\mathbf{A}\cdot\mathbf{p}+\mathbf{p}\cdot\mathbf{A})+\frac{e^2}{2mc^2}\,|\,\mathbf{A}\,|^2\,, \tag{1}$$

where $\mathbf{A}$ is the vector potential of the electromagnetic radiation. (We choose a gauge such that the scalar potential is zero.) The term in $|\,\mathbf{A}\,|^2$ leads to second-order processes (such as diamagnetism and light scattering) and will be neglected here. For photoemission the field $\mathbf{A}$ can be treated as a classical time-dependent perturbation, and results will be the same as if a proper quantum treatment had been made. For inverse photoemission, however, this is no longer true. Since photons are created it becomes necessary to quantize the electromagnetic field. In such a treatment the classical vector potential is replaced by the field operator $\mathbf{A}(\mathbf{x},t)$ defined by[4]

$$\mathbf{A}(\mathbf{x},t)=\frac{1}{(V_p)^{1/2}}\sum_{\mathbf{q}}\sum_{\alpha}c\frac{2\pi\hbar}{\omega}[a_{\mathbf{q},\alpha}(t)\hat{\epsilon}^{(\alpha)}e^{i\mathbf{q}\cdot\mathbf{x}}+a^{\dagger}_{\mathbf{q},\alpha}(t)\hat{\epsilon}^{(\alpha)}e^{-i\mathbf{q}\cdot\mathbf{x}}]\,, \tag{2}$$

 ©1985 The American Physical Society

where $\hat{\epsilon}^{(\alpha)}$, the linear polarization vector is a real unit vector whose direction depends on the photon propagation direction $\mathbf{q}$. The two operators $a^{\dagger}_{\mathbf{q},\alpha}$ and $a_{\mathbf{q},\alpha}$ either create or destroy a photon in the state $\mathbf{q},\alpha$, respectively. V_p is the normalization volume for the photon. For inverse photoemission the initial state consists of an electron in a continuum state $\psi_{\mathbf{k}}(\mathbf{r})$ with no photons and the final state consists of an electron in a bound state $\psi_b(\mathbf{r})$ and a photon with wave vector $\mathbf{q}$. Then the transition rate is given by Eqs. (1) and (2) using first-order perturbation theory:

$$R=\frac{2\pi}{\hbar}c^2\frac{2\pi\hbar}{\omega}\frac{1}{V_p}|\langle b|\hat{\epsilon}\cdot\mathbf{p}|\mathbf{k}\rangle|^2\rho_p\ , \tag{3}$$

where ρ_p is the photon density of states

$$\rho_p=\frac{Vp}{(2\pi)^3}\frac{\omega^2}{\hbar c^3}d\Omega \tag{4}$$

and $d\Omega$ is the solid angle of emission. Then

$$R=\frac{1}{2\pi}\frac{e^2}{\hbar c}\frac{\omega}{m^2c^2}|\langle b|\hat{\epsilon}\cdot\mathbf{p}|\mathbf{k}\rangle|^2 d\Omega\ , \tag{5}$$

where $e^2/\hbar c=\alpha\approx\frac{1}{137}$.

To obtain a cross section, we divide by the incident electron flux

$$j=\frac{\hbar k}{m}\frac{1}{V_e}\ . \tag{6}$$

We further assume that the continuum electron state is normalized to a box of volume V_e (which need not be the same as the photon normalization box). Then

$$\frac{d\sigma}{d\Omega}=\frac{\alpha}{2\pi}\frac{\omega}{mc^2}\frac{1}{\hbar k}|\langle b|\hat{\epsilon}\cdot\mathbf{p}|\mathbf{k}\rangle|^2\ . \tag{7}$$

It is interesting to compare this cross section with the one for photoemission using the same assumption. Now the final states are those of electrons, the density of states factor becoming

$$\rho_e=\frac{V_e}{8\pi^3}\frac{mk}{\hbar^2} \tag{8}$$

and the incident flux is the photon flux

$$j=\frac{\omega}{8\pi\hbar c}\frac{1}{V_p}\ . \tag{9}$$

Then

$$\frac{d\sigma}{d\Omega}=\frac{\alpha}{2\pi}\frac{k}{m}\frac{1}{\hbar\omega}|\langle\mathbf{k}|\hat{\epsilon}\cdot\mathbf{p}|b\rangle|^2\ . \tag{10}$$

Note that the ratio R of these two cross sections is

$$R=\left[\frac{d\sigma}{d\Omega}\right]_{\text{inv}}\Big/\left[\frac{d\sigma}{d\Omega}\right]_{\text{photo}}=\frac{\omega^2}{c^2k^2}=q^2/k^2$$

or

$$R=\left[\frac{\lambda_{\text{elec}}}{\lambda_{\text{phot}}}\right]^2\ . \tag{11}$$

That is, the ratio of the inverse photoemission cross section to that of photoemission is the ratio of the square of the wavelength of the electron to that of the photon. At energies characteristic of the UV range, for instance 10 eV, the inverse photoemission cross section is smaller by $\approx 10^5$ from the photoemission cross section. At the higher energies, of the order of 1000 eV, characteristic of x-ray photoelectron spectroscopy or bremsstrahlung isochromat spectroscopy the cross sections differ by a factor of 10^3.

The cross sections are only related in this way if the matrix elements are the same (or differ by sign). This is not generally true because in photoemission an electron is removed from the system while in inverse photoemission an electron is added to the system. For example, the photoemission cross section of an atom is related to the inverse cross section of its positive ion by Eq. (11) but the inverse cross section for the neutral atom bears no special relation to the photoemission cross section for that atom. The difference depends on the degree of localization of the states. For a band state in a solid the removal or addition of an electron is presumably equivalent and again Eq. (11) holds.

In all of these expressions we have assumed that the states $\psi_{\mathbf{k}}$ and ψ_b satisfy a one-electron Schrödinger equation

$$-\frac{\hbar^2}{2m}\nabla^2\psi+V\psi=\epsilon\psi\ . \tag{12}$$

If the potential $V(r)$ falls off more rapidly than $1/r$ at large distances then for photoemission the continuum states $\psi_{\mathbf{k}}$ have the form of plane waves plus incoming spherical waves[5]

$$\psi_{\mathbf{k}}(\mathbf{r})\sim e^{i\mathbf{k}\cdot\mathbf{r}}+f\frac{e^{-ikr}}{r}\quad\text{as } r\to\infty\ . \tag{13a}$$

The inverse process requires

$$\psi'_{\mathbf{k}}(\mathbf{r})\sim e^{i\mathbf{k}'\cdot\mathbf{r}}+f\frac{e^{+ik'r}}{r}\quad\text{as } r\to\infty\ , \tag{13b}$$

That is, a plane wave plus outgoing spherical waves. Usually $\mathbf{k}$ is chosen to be in the direction of the electron detector while $\mathbf{k}'$ points from the electron source towards the sample. If the matrix element for photoemission is given by

$$M(\mathbf{k})=\langle\mathbf{k}|\hat{\epsilon}\cdot\mathbf{p}|b\rangle$$

and that for inverse photoemission

$$M'(\mathbf{k}')=\langle b|\hat{\epsilon}\cdot\mathbf{p}|\mathbf{k}'\rangle\ .$$

Then, provided the bound-state wave function is real, it can be shown that

$$M(\mathbf{k})=-M'(-\mathbf{k}')\ ,$$

and therefore the photoemission matrix elements may be used for inverse photoemission provided the direction is taken from sample to electron source rather than vice versa.

A second point concerns the potential used to calculate these states. For photoemission the potential is asymptotically $-e^2/r$ so that the expressions (13a) and (13b) should be replaced by Coulomb wave functions. For in-

verse photoemission the problem is analogous to electron scattering for which at large r the potential behaves like $-\alpha_{\rm pol}/r^4$, where $\alpha_{\rm pol}$ is the polarizability of the atom or molecule.[6] Then Eqs. (13a) and (13b) are correct asymptotically. This illustrates again that the matrix elements for photoemission and its inverse are not precisely the same.

Photoemission cross sections are usually not strongly dependent on the potential at large distances. However, as noted by Wigner[7] and others[8] the behavior near threshold depends critically on the long-range part of the potential. For example, if this potential is Coulombic then the photoemission cross section is finite at threshold resulting in an absorption edge. Applying the rule, Eq. (11), that the inverse photoemission cross section is q^2/k^2 times the photoemission cross section we see that the inverse cross section will therefore diverge as $k \to 0$. However, for potentials which go to zero more rapidly at large distances the threshold behavior is more complex. Using Wigner's threshold laws it can be shown that the threshold cross section for photodetachment (photoemission from negative ions) has the form

$$\sigma \approx k^{2l+1} ,$$

where l is the angular momentum of the continuum electron. From Eq. (11) we therefore find that the threshold cross section for the time-reversed process, inverse photoemission, would be k^{2l-1}. As a result, the inverse photoemission cross section into an s state, which could only come from a p-type continuum state will vanish at threshold as k but the inverse cross section into a p state, which can come from s continuum states will diverge as k^{-1}.

Molecules have been considered by Geltman and coworkers[8] who have shown that for transitions into σ or π states of heternuclear diatomic molecules the inverse cross section will diverge as k^{-1}. This may be viewed as a consequence of the fact that s continuum waves participate in transitions into σ or π bound states and for such states the atomic threshold law applies. In practice deviations from these threshold laws may occur at extremely low energies. For example, for the CO 2π level discussed below even at a kinetic energy of ≈ 0.1 eV the cross section is dominated by the p continuum state (not s) so no divergence is apparent at that energy.

III. MULTIPLE-SCATTERING THEORY

We use multiple-scattering theory to calculate the initial and final states for oriented molecules. In this approach a potential which consists of nuclear attraction, Coulomb repulsion, and a local exchange-correlation contribution is sphere and volume averaged to the muffin-tin form. The details have been given in Ref. 9.

It is convenient to use the acceleration form of the matrix element based on the fact that

$$\langle f \,|\, \mathbf{p} \,|\, i \rangle = (i/\omega) \langle f \,|\, \nabla V \,|\, i \rangle$$

so that

$$\left[\frac{d\sigma}{d\Omega} \right]_{\rm inv} = \frac{\alpha}{2\pi} \frac{1}{mc^2} \frac{1}{\hbar\omega k} \,|\, \langle b \,|\, \hat{\epsilon} \cdot \nabla V \,|\, \mathbf{k} \rangle \,|^2 . \qquad (14)$$

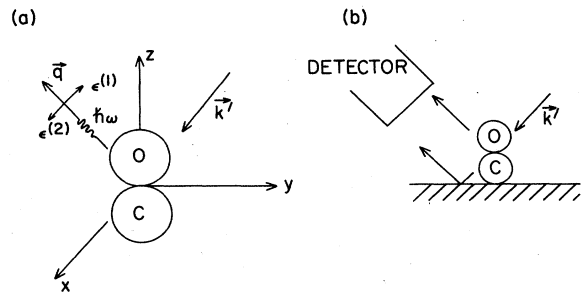

FIG. 1. Schematics of the models used for the calculation showing (a) the microscopic detail of the orientation of the molecule and the incident and exit angles of the electron and photon, respectively, and (b) the macroscopic detail showing the inclusion of the dielectric response of the substrate.

The most general form of the angular dependence of the matrix element is

$$\langle \mathbf{k} \,|\, \hat{\epsilon} \cdot \nabla \,|\, b \rangle = \sum_{\nu,l,m} \frac{4\pi}{3} Y_{1\nu}(\hat{\epsilon}) F_{\nu lm} Y_{lm}(\hat{\mathbf{k}}) , \qquad (15)$$

where the Y's are spherical harmonics and $\mathbf{k}$ points from electron source toward the molecule.

The total cross section for a gas-phase molecule is obtained by squaring, integrating over $\hat{\epsilon}$, and averaging over $\hat{\mathbf{k}}$. There is also a factor of 2 for the two possible polarizations:

$$\sigma = \frac{\alpha}{2\pi} \frac{1}{mc^2} \frac{1}{\hbar\omega k} \sum_{\nu,L} 2 \frac{4\pi}{9} \,|\, F_{\nu L} \,|^2 . \qquad (16)$$

Figure 1(a) shows a schematic of the microscopic details of the calculation. The molecular cluster is oriented along the z axis and the electron is incident in the y-z plane. The potentials were constructed by performing self-consistent calculations using the Gunnarsson-Lundquist form for exchange plus correlation.

In Fig. 2 the total cross sections calculated from Eq. (16) is shown both for a free carbon monoxide molecule and a carbon monoxide molecule linearly bonded to a pal-

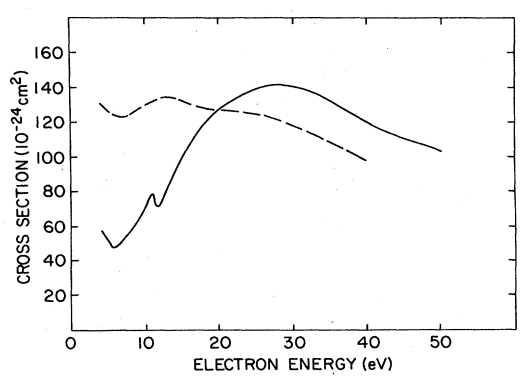

FIG. 2. Calculated total cross section for the emission of photons as a function of incident electron energy for a carbon monoxide molecule (dashed line) and a carbon monoxide palladium cluster (solid line).

TABLE I. Atomic radii (bohr) and calculated molecular-orbital binding energies (rydbergs) for carbon monoxide and palladium carbon monoxide clusters.

$r_c=1.15$	$r_0=0.98$ CO	$r_{Pd}=2.59$ Pd-CO
2π	-0.3198	-0.4192
5σ	-0.6902	-0.9466
1π	-1.0411	-0.9549
4σ	-1.0848	-1.1975

ladium atom via the carbon atom. The radii used for the carbon, oxygen, and palladium atoms are given in Table I where we also show the calculated binding energies of the various molecular orbitals for the two clusters. It should be emphasized that these calculations are ground-state or neutral-atom calculations. It will be seen in Fig. 2 that both calculations have essentially the same features and in particular both show structure in the region of 12.5-eV electron kinetic energy which is partly associated with the "shape resonance" frequently observed in photoemission as a final-state effect.[10]

The calculations shown in Fig. 2 employed a Coulomb potential at large distances. As already stated in Sec. II, such a potential is not strictly applicable to the inverse photoemission process where the incoming electron approaches a neutral molecule.

Figure 3 shows a comparison of the total cross section for the emission of photons calculated for a free carbon monoxide molecule both with and without the Coulomb potential. It shows that at higher photon energies both calculations produce similar results and thus equations relating cross sections of the form of Eq. (11) may be used with reasonable accuracy. However, below approximately four times the threshold energy such relations should be used with caution.

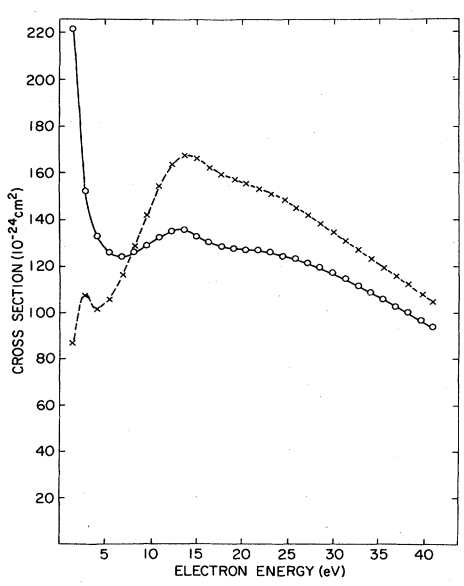

FIG. 3. Calculated total cross section for the emission of photons as a function of incident electron energy for a carbon monoxide molecule using a Coulombic potential (—○—○—) and a neutral atom potential (—×—×—×—).

In order to facilitate comparisons between experiment and theory for adsorbed molecules, we have also included the reflective properties of the metal substrate and the refraction of the incident electron. Both of these effects have previously been considered in different photoemission calculations[11] but the low energies (e.g., 9.7 eV) characteristic of many inverse photoemission experiments suggest that their inclusion will be important in the present calculation.

Refraction of the incident electron is accounted for simply by noting that in crossing the vacuum level the parallel component of momentum is conserved, thus

$$E_1^{1/2}\sin\theta_1=(E_2+W)^{1/2}\sin\theta_2 .$$

Here E_1 and θ_1 are the energy and incident angle in the vacuum and E_2 and θ_2 are the energy and angle within the molecule. W is the inner potential which we have taken to be 11 eV.

To take account of the dielectric properties of the metallic substrate we consider either the possibility of a photon traveling directly from the emitting molecule to the detector or also the possibility of a photon undergoing a reflection at the surface before traveling to the detector, as illustrated in Fig. 1(b). Consideration of the effects of reflection on the different components of the "classical" vector potential leads us to an effective vector potential at the molecule identical to that derived from Fresnel's equations for the equivalent situation in photoemission. Thus

$$\epsilon_x=(1+r_s)\epsilon_x=\epsilon^{(2)} ,$$

$$\epsilon_y=(1-r_p)\epsilon_y=\epsilon^{(1)}\sin\theta ,$$

$$\epsilon_z=(1+r_p)\epsilon_z=\epsilon^{(1)}\cos\theta ,$$

where r_s and r_p define the reflectivities of light with its vector potential perpendicular and parallel to the scattering plane, respectively. In the present case the scattering plane is the y-z plane.

In the preceding section it was shown that the total cross section for emission of photons showed structure characteristic of the σ shape resonance. This effect is more clearly demonstrated if one examines the differential cross section relating to the emission of photons for electrons incident along the molecular axis.

Figure 4 shows a calculation of such a differential cross section for the simple carbon monoxide cluster for two different potentials. We have published a similar curve for the palladium carbon monoxide cluster previously.[12] It will be seen that at lower photon energies there exists a well-defined peak in the cross section, which results from the incoming electron being scattered into a number of channels and in particular at these low photon energies into the σ channel. From this channel there is a high cross section for transitions into the unoccupied 2π level of the molecule.

We explored the effect of this resonance in our earlier publication[12] where we examined the cross section for the emission of photons as a function of the angle of incidence of the electrons at photon energies characteristic

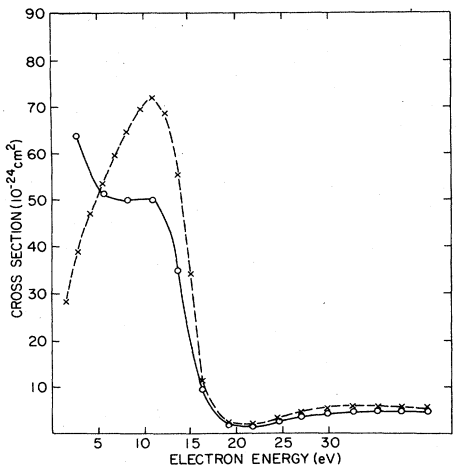

FIG. 4. Calculated cross-section for the emission of photons for normally incident electrons as a function of electron energy using a Coulombic potential (—O—O—O—) and a neutral-atom potential (—X—X—X—).

of the resonance. It was found that on resonance the differential cross section peaks for normally incident electrons whereas off resonance the cross section is strongest for electrons that have grazing incidence or high angles with respect to the molecular axis.

IV. CONCLUSIONS

In the past it has been common practice to compare angle-resolved photoemission experiments from adsorbed molecules with calculations on the oriented gas-phase molecule. In Sec. III it was shown that the equivalent comparison in inverse photoemission will give poor results for low photon energies or photon energies less than approximately four times the threshold energy (threshold energy equals binding energy of the final bound state). This unfortunate result stems from the fact that the wave function used to describe the final state in photoemission is not appropriate to the initial state of inverse photoemission. However it should be noted that within the solid-state environment screening or delocalization will make the two processes more equivalent. Thus in photoemission the outgoing electron will experience a "neutralized" ion and in inverse photoemission the incoming electron will experience the potential of a neutral atom. With this limitation in mind we have demonstrated in this paper the use of a quantum-theoretical treatment to calculate "photon-emission" cross sections in inverse photoemission. These calculations have shown that it should be possible to observe shape-resonance effects in inverse photoemission as previously observed in photoemission. However, no attempt has been made here to calculate the precise energy position of this resonance which will show a strong dependence on the type of potential used.

The fact that it is possible to observe transitions from the σ resonance to the unoccupied 2π level suggests that it may be possible to measure bond lengths of adsorbed molecules. In a number of papers on core excitation of adsorbed molecules it has been shown that the position of the shape resonance shows a marked dependence on the bond length of the adsorbed molecule.[13]

The use of inverse photoemission as another monitor of bond lengths may be hampered by the fact that to observe such resonances one requires tunable photon detectors in a range where such devices may be least efficient. Second, because of the low photon energies, more careful consideration of the dielectric response of the substrate must be given compared with that appropriate to the high energies characteristic of core-level spectroscopies.

ACKNOWLEDGMENT

This work was supported by the Division of Materials Sciences, U.S. Department of Energy under Contract No. DE-AC02-76CH00016.

[1]V. Dose, Prog. Surf. Sci. **13**, 225 (1983); N. V. Smith, Vacuum **33**, 803 (1983).
[2]P. A. M. Dirac, Proc. R. Soc. London, Ser. A **114**, 243 (1927).
[3]J. B. Pendry, J. Phys. C **14**, 1381 (1981).
[4]See, for example, J. Sakurai, Advanced Quantum Mechanics (Addison-Wesley, Reading, PA, 1967).
[5]M. Gell-Mann and M. L. Goldberger, Phys. Rev. **91**, 398 (1953).
[6]J. W. Davenport, W. Ho, and J. R. Schrieffer, Phys. Rev. B **17**, 3115 (1978).
[7]E. P. Wigner, Phys. Rev. **73**, 1002 (1948).
[8]L. M. Branscomb, D. S. Burch, S. J. Smith, and S. Geltman, Phys. Rev. **111**, 504 (1958); T. F. O'Malley, *ibid.* **137**, A1668 (1965).
[9]J. W. Davenport, G. J. Cosgrove, and A. Zangwill, J. Chem. Phys. **78**, 1095 (1983).
[10]J. W. Davenport, Phys. Rev. Lett. **36**, 945 (1976).
[11]M. Scheffler, K. Kambe, and F. Forstemann, Solid State Commun. **25**, 93 (1978).
[12]P. D. Johnson, D. A. Wesner, J. W. Davenport, and N. V. Smith, Phys. Rev. B **30**, 4860 (1984).
[13]F. Sette and J. Stöhr, in *EXAFS and Near Edge Structure III*, edited by K. O. Hodgson, B. Hedman, and J. E. Penner-Hahn (Springer, Berlin, Heidelberg, New York, 1984), p. 250.